

Nanoelectromechanical rotary current rectifier

Christopher W. Wächtler^{1,*}, Alan Celestino,¹ Alexander Croy², and Alexander Einfeld¹¹Max Planck Institute for the Physics of Complex Systems, Nöthnitzer Strasse 38, 01187 Dresden, Germany²Institute for Materials Science and Max Bergmann Center of Biomaterials, TU Dresden, 01069 Dresden, Germany

(Received 21 March 2021; revised 7 June 2021; accepted 12 July 2021; published 27 July 2021)

Nanoelectromechanical systems (NEMS) are devices integrating electrical and mechanical functionality on the nanoscale. Because of individual electron tunneling, such systems can show rich self-induced, highly nonlinear dynamics. We show theoretically that rotor shuttles, fundamental NEMS without intrinsic frequencies, are able to rectify an oscillatory bias voltage over a wide range of external parameters in a highly controlled manner, even if subject to the stochastic nature of electron tunneling and thermal noise. Supplemented by a simple analytic model, we identify different operational modes of charge rectification. Intriguingly, the direction of the current depends sensitively on the external parameters.

DOI: [10.1103/PhysRevResearch.3.L032020](https://doi.org/10.1103/PhysRevResearch.3.L032020)

Introduction. Rapidly growing technological abilities have resulted in fabricating devices with sizes below micrometers [1–7]. The ability to control charge transport is crucial for the design of such devices. One basic functionality is current rectification, i.e., the regulation of the preferential direction of the current resulting from an oscillatory bias voltage. This phenomenon is based on nonlinear current-voltage characteristics. Paradigmatic candidates are nanoelectromechanical systems (NEMS), which combine mechanical and electronic degrees of freedom in a single nanoscale device [8–11]. So-called electron shuttles are particular examples of NEMS, where a movable island transfers electrons between two leads to which it is tunnel-coupled [12–19]. Notably, the rate of tunneling depends on the position of the shuttle, which allows for self-induced dynamics. Hence, electron shuttles are interesting candidates to investigate rectification because they do not require any active regulation from the outside.

Different realizations of electron shuttles include a harmonic oscillator [12,20,21] or a rotor [22–26] to which the island is attached. While the dynamics of the former are mainly determined by the intrinsic frequency of the oscillator, the lack of such a frequency in the latter leads to complex and rich dynamics, which allow the rotor to act as a motor, sensor, or electron pump [25,26]. Such a rotor could be realized by molecules on a surface [27–37] or an electronic island mounted onto a rigid rotor.

While for the oscillator-based shuttle it has been shown that it is possible to rectify an oscillating signal [21,38] it is not obvious whether rectification can still occur without such an

intrinsic oscillatory frequency, especially in the presence of thermal noise.

Here we demonstrate at the example of a rotor shuttle that the existence of an intrinsic eigenfrequency is in general not required for NEMS to be able to rectify an oscillating current. The rectification works over a wide range of external voltage bias magnitudes and frequencies. The rotor dynamics show a complex pattern of various operational modes which very sensitively depends on the external parameters like friction and driving amplitude; for the same external frequency, even different directions of the current are possible. From our extensive numerical simulations, which take into account both the stochastic nature of the tunneling as well as thermal fluctuations, a clear picture of this dependence emerges and is supplemented by a simple analytic model.

Model. The single electron rotor, shown in Fig. 1(a), consists of a single electron transistor where the central island (e.g., a quantum dot) is mounted onto a rotor [25,26]. The position of the island is specified by the angle θ . The rightmost position is taken as $\theta = 0$ [cf. Fig. 1(a)]. The island is subject to an electrostatic torque

$$\mathcal{T}_{\text{el}}(\theta, q, t) = -qE(t) \sin(\theta). \quad (1)$$

Here q denotes the charge of the island, which we express in units of the electron charge. The time-dependent electric field $E(t)$ is caused by a time-dependent bias voltage $E(t) = \alpha V_0 \sin(\omega_d t)$, with driving frequency ω_d , amplitude V_0 , and α a constant factor.¹ We assume the limit of strong Coulomb blockade [39–41], such that the island is either empty ($q = 0$) or occupied by exactly one (excess) electron ($q = 1$). This approximation is justified in the case of low temperatures, $\beta \gg 1/E_C$ (E_C being the charging energy of the island), and voltages, $|V_0| \ll E_C$.

¹Approximately, $\alpha \propto 1/d$ with d being the distance between the electrodes.

*cwaechtler@pks.mpg.de

Published by the American Physical Society under the terms of the Creative Commons Attribution 4.0 International license. Further distribution of this work must maintain attribution to the author(s) and the published article's title, journal citation, and DOI. Open access publication funded by the Max Planck Society.

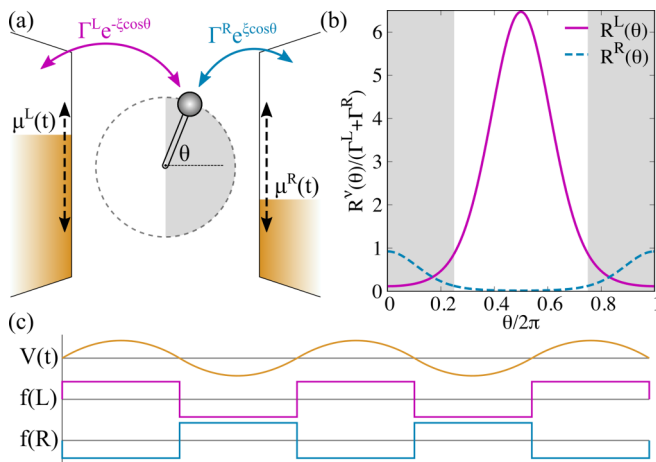


FIG. 1. (a) Pictorial drawing of a rotor shuttle driven by time-dependent chemical potentials $\mu^L(t)$ and $\mu^R(t)$. (b) Tunneling rate functions $R^L(\theta)$ and $R^R(\theta)$ between system and left (magenta solid) and right (blue dashed) lead as a function of θ . (c) Schematic time dependence of the oscillating voltage $V(t)$ (top) and the corresponding left (middle) and right (bottom) Fermi functions. Parameters: $\Delta = 0.75$, $\xi = 2.0$.

Electrons can tunnel between the island and the left ($v = L$) and right ($v = R$) lead with rate functions $R_{q \rightarrow q'}^v(\theta)$, which depend exponentially on the position of the island and on the Fermi function of the respective lead. Specifically, we model the rate functions as

$$\begin{aligned} R_{0 \rightarrow 1}^v(\theta, t) &= R^v(\theta) f^v[-E(t) \cos(\theta)], \\ R_{1 \rightarrow 0}^v(\theta, t) &= R^v(\theta) \{1 - f^v[-E(t) \cos(\theta)]\}. \end{aligned} \quad (2)$$

Here $R^L(\theta) = \Gamma^L \exp[-\xi \cos(\theta)]$ and $R^R(\theta) = \Gamma^R \exp[\xi \cos(\theta)]$ with dimensionless tunneling length ξ [24] contains the exponential dependence of the tunnel rates. The Fermi function $f^v[\varepsilon] = \{1 + \exp[\beta(\varepsilon - \mu^v)]\}^{-1}$ contains the inverse temperature β and the charging energy of the island $[-E(t) \cos \theta]$, and essentially determines the direction of tunneling via the time-dependent chemical potentials $\mu^L(t) = V_0 \sin(\omega_d t)/2$ and $\mu^R(t) = -V_0 \sin(\omega_d t)/2$.² For our choice of parameters, $f^L[\varepsilon] \approx 1$ during the first half of the driving period [$t \in (0, T/2)$] and $f^L[\varepsilon] \approx 0$ during the second half [$t \in (T/2, T)$], and the opposite for the right lead. Thus, electron tunneling is unidirectional with opposite directions during the first and second half of the driving period, respectively. We provide further details on the specifics of electron tunneling in Sec. I of the Supplemental Material [42].

We model the effects of thermal noise on the rotor motion via Langevin dynamics. For individual trajectories the charge q_t changes stochastically by means of a Poisson process determined by the tunneling rate functions (2) [42]. We denote a stochastic process by a subscript t in the following. For a rotor with moment of inertia I subject to friction with friction constant γ and the electrostatic torque $\mathcal{T}_{el}(\theta, q, t)$, the stochastic

equations of motion take the form [26,43]

$$\begin{aligned} d\theta_t &= \omega_t dt, \\ I d\omega_t &= [-\gamma \omega_t + \mathcal{T}_{el}(\theta_t, q_t, t)] dt + \sqrt{2\gamma/\beta} dB_t, \\ dq_t &= \sum_v dq_t^v = \sum_{vq'} (q' - q_t) dN_{q' \rightarrow q_t}^v(\theta_t, t). \end{aligned} \quad (3)$$

The Wiener increment dB_t has zero mean ($\mathbb{E}[dB_t] = 0$) and variance $\mathbb{E}[dB_t^2] = dt$, where $\mathbb{E}[\bullet]$ denotes an average with respect to many realizations of a stochastic process. The Poisson increments $dN_{q' \rightarrow q_t}^v(\theta_t, t) \in \{0, 1\}$ obey the statistics $\mathbb{E}[dN_{q' \rightarrow q_t}^v(\theta_t, t)] = R_{q' \rightarrow q_t}^v(\theta_t, t) dt$ and $dN_{q' \rightarrow q_t}^v(\theta_t, t) dN_{q'' \rightarrow q_t}^v(\theta_t, t) = \delta_{v\bar{v}} \delta_{q_i \bar{q}_i} dN_{q' \rightarrow q_t}^v(\theta_t, t)$. Specifics on the numerical implementation can be found in Sec. II of the Supplemental Material [42]. Note that the system dynamics described by Eq. (3) can equivalently be expressed by a generalized Fokker-Planck equation, where electron tunneling is accounted for by means of a master equation with rate functions specified by Eq. (2) [44].

To quantify rectification we use the (averaged) electron current, which is defined by the difference in the number of electrons moving to and from the right lead.³ A positive current corresponds to electrons tunneling from the island into the right lead ($dq_t^R = 1$) and a negative current corresponds to the opposite direction ($dq_t^R = -1$). We thus calculate the current averaged as

$$\langle J \rangle \equiv \frac{1}{t_f - t_i} \int_{t_i}^{t_f} dq_t^R dt, \quad (4)$$

where $\langle \bullet \rangle$ denotes a time average of a stochastic process. Herein, the time interval $t_f - t_i$ is defined in terms of the starting time t_i and the final time t_f . We choose the starting time t_i and the interval $t_f - t_i$ large enough such that transient dynamics can be ignored and the current has sufficiently converged [42]. Furthermore, we have checked numerically that the time-averaged current $\langle J \rangle$ defined in Eq. (4) is equivalent to the average over many realizations of the stochastic process ($\mathbb{E}[J]$) and that it is independent of initial conditions.

Rectification. Breaking the left-right symmetry of the rotor shuttle is crucial for rectification to occur. We achieve such an asymmetry by choosing different tunneling rates for the left and the right lead. The asymmetry is characterized by

$$\Delta = \frac{\Gamma^L - \Gamma^R}{\Gamma^L + \Gamma^R}. \quad (5)$$

This asymmetry parameter has a range $-1 \leq \Delta \leq 1$ and, in the fully symmetric case, $\Delta = 0$. In the following we choose $\Delta = 0.75$ to obtain a pronounced asymmetry in the tunneling rates. As is clearly visible in Fig. (b), for our parameters, one has the following situation: When the island is close to the left lead, it is essentially *decoupled* from the right lead and thus current through the system in either direction is significantly decreased. In the opposite case, when the island is close to the right lead (gray area) it is still coupled to the left lead (with a similar strength as to the close-by right lead) such

²The system is biased symmetrically around the bare island energy such that the Fermi functions do not depend on it.

³However, the definition of the current with respect to the left lead is equivalent up to a sign because of particle conservation.

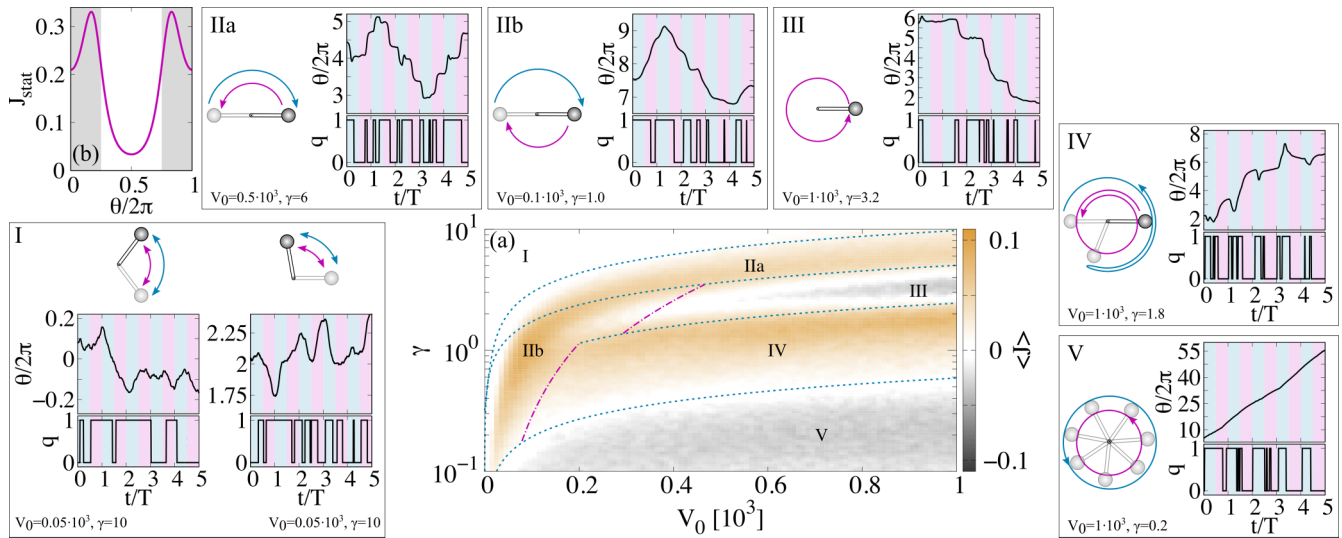


FIG. 2. (a) Time-averaged current as a function of the driving strength V_0 and the friction γ , where a positive value (gold) indicates rectification from left to right and a negative value (silver) from right to left. The surrounding panels show exemplary excerpts of stochastic trajectories within regimes I–V together with schematic representations of the rotor dynamics during the first (blue arrow) and second (magenta arrow) half cycle of the driving. The dashed lines mark the borders of the individual regimes according to our analytic model. (b) Static current, when the rotor is held at a fixed angle θ . The electron current is calculated according to Eq. (4). Parameters of the system are $\Delta = 0.75$, $\omega_d = 1.6$, $\xi = 2.0$, $\beta = 5.0$, $\alpha = 0.1$, and $I = 1.0$.

that a current via electron tunneling is possible. Thus, in a static situation where the island is held at a fixed position rectification cannot occur.

The presence of multiple timescales—the driving frequency ω_d , the timescale of electron tunneling characterized by the functional form of $R^L(\theta)$ and $R^R(\theta)$ and finally the timescale of rotation, which depends on γ as well as on V_0 —promotes the rich dynamics of the rotor shuttle. For now, we focus on the regime where the driving frequency is comparable to the smaller electron tunneling rate, which mainly determines the electronic dynamics. We make remarks on the cases of slow and fast driving at the end of this Letter. In the following, we specify $\omega_d/R^R(0) = 0.86$ with $\xi = 2$ and analyze the impact of friction and driving strength on the system dynamics and rectification.

In the central panel of Fig. 2 we show the averaged current $\langle J \rangle$ as a function of the bias voltage V_0 and the friction γ . In the gold shaded areas the net current is positive, i.e., on average from left to right. In the silver shaded areas it is negative. We see that rectification can be obtained over a wide range of parameters. To understand the complex dependence on the parameters, it is instructive to analyze the underlying dynamics of the rotor. We have identified several regions with distinct dynamic features. These regions are marked I–V in the figure and representative trajectories are provided in the surrounding panels.

In region I there are two different dynamics, which both produce no net current: for small V_0 the island is (most of the time) located close to the right lead. As mentioned above, in this situation rectification is not possible because the island remains coupled to both leads at all times. For larger V_0 the rotor is still mostly in the vicinity of the right lead. However, during the second half cycle (when the electric fields points from right to left) the island may move towards the left lead and pass the upper-right (lower-right) position, where one electron

has been shuttled. As the electric field changes direction, the island returns to the right lead and also shuttles one electron (from left to right). Thus, also in this situation rectification does not occur.

By decreasing the friction and/or increasing the driving strength, one enters region II. Here, the rotor motion is characterized by switching from left to right and vice versa during the first and second half of the driving period, respectively. In IIa these half rotations are fast compared with the driving frequency such that the island remains very close to one lead for about a quarter of the driving period. In IIb (smaller friction and smaller driving strength compared with regime IIa) the rotor turns slowly and approximately performs half a rotation during one half cycle of the driving. In both cases, due to the asymmetry in the tunneling rates, electron tunneling is significantly decreased in the second half cycle, resulting in an overall positive current.

In region III the rotor remains close to the right lead during the first half of the driving period and completes one (or even two) full revolutions during the second half. Thus, in this regime the system alternates between a static and a moving mode synchronized to the driving frequency. During the full revolutions, typically one electron is shuttled from right to left producing a current of $J_{\text{revolution}} = -\omega_d/\pi$, which is larger than the current via electron tunneling in the static phase [cf. Fig. 2(b)]. Hence, there is a negative net current in this regime.

Region IV shows an intriguing interplay between friction and driving strength: During the first half cycle the island typically moves toward the right lead, passes the closest position, loses its electron, is slowed down by friction, picks up another electron from the left lead, changes direction, and approaches the right lead again. During this process *two* electrons have been shuttled from left to right. As the electrostatic field switches, the rotor performs one and a half rotations before arriving in the proximity of the left lead, which blocks

further electron tunneling. This results in a positive average current.

Lastly, in region V the friction γ is small, resulting in continuous rotational motion with high angular velocity.⁴ If the rotor would rotate with the same angular velocity during the first and second half cycle, the island would be located equally close to the right as to the left lead without rectification. However, we find that the island is mostly occupied by an electron during the first half cycle, such that the rotor is accelerated while turning toward the right lead. Due to the high angular velocity and the small tunneling rate, the occupied rotor passes the rightmost position and is decelerated by the electrostatic torque and friction. Hence, the island during the first half cycle spends effectively more time close to the left lead. On the other hand, during the second half cycle an electron on the island quickly tunnels out such that the rotor is constantly slowed down by friction, which allows for another electron to be shuttled from right to left. The uneven rotations result in an overall negative current.

Analytic model. From the above discussion it is apparent that the capability and direction of rectification is intimately connected to the rotational dynamics of the system. Here, the possibility of the rotor to switch between left and right positions is of great importance due to asymmetry in the tunneling rates. While electrons can tunnel through the system along the bias when the island is closer to the right lead, current is significantly decreased when closer to the left lead. Furthermore, the interplay of multiple timescales and the presence of thermal noise contribute to the rich and complex rectification mechanism. In the following we develop a basic model of the rotor shuttle, which includes the most important features of the rectifier and promotes a clear understanding of the rectification mechanism.

The average current mainly depends on the rotor dynamics during the second half of the driving oscillation. Consequently, of particular importance is the maximum angle θ_{\max} that the island can reach. From now on we discuss the rotor dynamics during the second half cycle when the empty island is initially located at $\theta = 0$. As an electron tunnels into the island from the right ($q = 1$) the electrostatic torque accelerates the rotor until, at $\theta = \pi/2$, the electron tunnels out of the island into the left lead. After this jump, the rotor has an angular velocity of ω_{jump} such that, during the remaining time of the second half cycle, the empty island ($q = 0$) continues to rotate while being decelerated due to friction until it stops at a final angle θ_{maxfin} . We approximate this remaining time by $t_{\text{remain}} = T(\theta_{\max} - \pi/2)/2\theta_{\max}$. Additionally, the rotor performs a rotation $\theta_{\text{diffusive}} = \sqrt{2t_{\text{remain}}/\gamma\beta}$ due to diffusion during this time span. The maximum angle the rotor can reach is then given by $\theta_{\max} = \theta_{\text{maxfin}} + \theta_{\text{diffusive}}$, which is the central equation to approximate the transitions between the different rectification regimes.

We now need to determine θ_{maxfin} . To this end, we turn to Newton's equation of a deterministic damped rotor, $I\ddot{\theta} = -\gamma\dot{\theta}$ with an initial position $\theta = \pi/2$ and an initial angular

⁴The system rotates for long times in one direction but may abruptly change directions and turn the opposite way for many cycles.

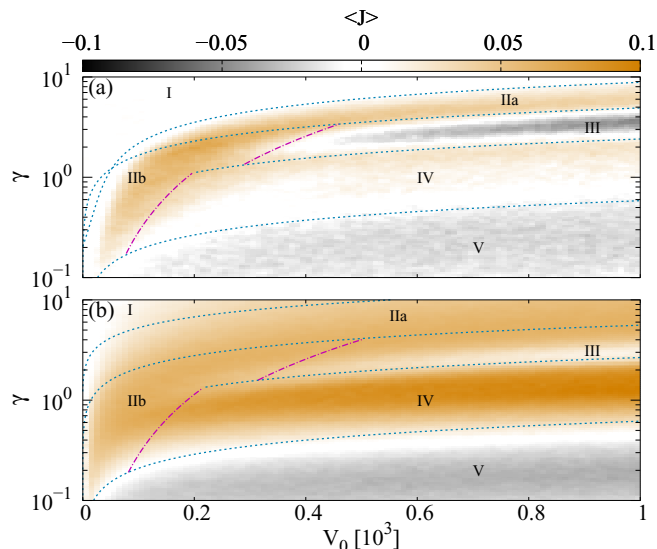


FIG. 3. Time-averaged current for (a) fast driving ($\omega_d = 2.5$) and (b) slow driving ($\omega_d = 0.4$) compared with Fig. 2. The dashed lines mark the borders of the individual regimes according to our analytic model. The electron current is calculated according to Eq. (4). Parameters of the system are $\Delta = 0.75$, $\xi = 2.0$, $\beta = 5.0$, $\alpha = 0.1$, and $I = 1.0$.

velocity equal to the angular velocity ω_{jump} after the electron has tunneled out of the system. The final angle is then given by $\theta_{\text{maxfin}} = \pi/2 + \omega_{\text{jump}}/\gamma$. To estimate the angular velocity ω_{jump} at which the electron has tunneled we set the kinetic energy $E_{\text{kin}} = I\omega_{\text{jump}}^2/2$ equal to the difference in potential energy of a $\pi/2$ rotation of the occupied island, which we approximate as $\Delta E_{\text{el}} = \alpha V_0 [1 - \cos(\pi/2)]$.

Within this model, the transitions between the different dynamic regimes are now solely determined by θ_{\max} , which are for $I \leftrightarrow II$, $\theta_{\max} = 5\pi/6$; for $II \leftrightarrow III$, $\theta_{\max} = 3\pi/2$; for $III \leftrightarrow IV$, $\theta_{\max} = 5\pi/2$; and for $IV \leftrightarrow V$, $\theta_{\max} = 17\pi/2$. We mark these transitions as blue dotted lines in the central panel of Fig. 2.

However, in regime III thermal noise may prevent the rotor from approaching the right lead: When the electrostatic torque is large enough to turn the island one full rotation—such that it would end up at the right-most position—but the thermal noise is able push the rotor $\pi/2$ forward or backward, the island ends up on the left side again (regime IIb). In this case, the thermal energy $E_{\text{thermal}} = \sqrt{2\gamma/\beta}2\pi = \langle E_{\text{el}} \rangle$, where $\langle E_{\text{el}} \rangle = 2\alpha V_0/\pi$. Similarly, the boundary of IV and IIb is given $E_{\text{thermal}} = \sqrt{2\gamma/\beta}3\pi = \langle E_{\text{el}} \rangle/2$. These transitions are marked as magenta dashed lines in Fig. 2.

Driving Frequency. Increasing the driving frequency ω_d has two important consequences: as long as the rotor can follow the driving frequency, in principle more electrons can be transferred per unit time via shuttling. However, electrons have now less time to tunnel, and the rotor has less time to reach its critical angle before the field switches again. As shown in Fig. 3(a), this mostly affects regimes III and IV where rectification stems from the delicate interplay of shuttling and tunneling. In regime III rectification increases as fewer electrons tunnel during the first half cycle, while in regime IV rectification decreases as consecutive transport of

two electrons during the first half cycle becomes less likely. Upon further increase of the driving frequency, the rotor cannot follow the fast changes of driving direction anymore making rectification no longer possible.

In contrast, for slow driving [cf. Fig. 3(b)] more electron-tunneling events can occur during each half cycle, which enhances rectification in regimes IIa and III. Similarly, for larger V_0 in regime I, the switching of the rotor from one side to the other induces rectification for slow driving. However, in regime III the slow driving decreases the current given by shuttling of one electron during a full revolution $J_{\text{revolution}} = -\omega_d/\pi$ such that the net current becomes positive.

For both cases—fast and slow driving—our analytic model approximates the different rectification scenarios very well, which reaffirms the intimate relation between rectification and rotor dynamics.

Conclusions. We have shown that, for a charge shuttle with rotational degree of freedom and driven by a symmetrically oscillating external bias voltage, there exist parameter regimes with a preferred electron current direction. The direction and strength of the current depends in a complex way on the parameters of the rotor-shuttle as well as on external parameters such as temperature and driving frequency.

The basic mechanism of rectification is self-induced oscillations and rotations. It is remarkable that such a rectification behavior can be observed for a system without intrinsic oscillation frequency in contrast, for example, to charge shuttles

based on harmonic oscillators. The absence of such intrinsic frequencies causes a complicated response of the current strength and direction to parameter changes. Nevertheless, there exist extended regions with similar current. This makes the rotor shuttle a promising device as it is often hard to perfectly specify all system parameters in an experimental setup. As an application, one could imagine for example a switch that is sensitive to driving frequency or amplitude.

Based on the analysis of individual trajectories we found that different dynamical processes dominate within the various rectification regimes. From this understanding we obtained a fully analytic model, which is capable of predicting regime separations. Such analytic estimations will be helpful when searching for experimental implementation of such devices.

Moreover, with the present work we have demonstrated that a system without harmonic confinement can perform similar objectives as oscillator-based NEMS, even at finite temperature. This paves the way to study collective effects in more complex architectures, for example, synchronization in weakly coupled systems without intrinsic frequency.

Acknowledgments. We thank M.T. Eiles for fruitful discussions and for a careful reading of the paper. C.W.W. acknowledges support from the Max-Planck Gesellschaft via the MPI-PKS Next Step fellowship. A.E. acknowledges support from the DFG via a Heisenberg fellowship (Grant No EI 872/5-1).

-
- [1] D. Rugar and P. Grütter, Mechanical Parametric Amplification and Thermomechanical Noise Squeezing, *Phys. Rev. Lett.* **67**, 699 (1991).
 - [2] C. Joachim, J. K. Gimzewski, and A. Aviram, Electronics using hybrid-molecular and mono-molecular devices, *Nature (London)* **408**, 541 (2000).
 - [3] R. He, X. Feng, M. Roukes, and P. Yang, Self-transducing silicon nanowire electromechanical systems at room temperature, *Nano Lett.* **8**, 1756 (2008).
 - [4] A. Subramanian, A. R. Alt, L. Dong, B. E. Kratochvil, C. R. Bolognesi, and B. J. Nelson, Electrostatic actuation and electromechanical switching behavior of one-dimensional nanostructures, *ACS Nano* **3**, 2953 (2009).
 - [5] A. K. Naik, M. Hanay, W. Hiebert, X. Feng, and M. L. Roukes, Towards single-molecule nanomechanical mass spectrometry, *Nat. Nanotechnol.* **4**, 445 (2009).
 - [6] L. Oroszlány, V. Zólyomi, and C. J. Lambert, Carbon nanotube archimedes screws, *ACS Nano* **4**, 7363 (2010).
 - [7] S. T. Bartsch, A. Lovera, D. Grogg, and A. M. Ionescu, Nanomechanical silicon resonators with intrinsic tunable gain and sub-nW power consumption, *ACS Nano* **6**, 256 (2012).
 - [8] H. G. Craighead, Nanoelectromechanical systems, *Science* **290**, 1532 (2000).
 - [9] K. L. Ekinici and M. L. Roukes, Nanoelectromechanical systems, *Rev. Sci. Instrum.* **76**, 061101 (2005).
 - [10] R. Bustos-Marín, G. Refael, and F. von Oppen, Adiabatic Quantum Motors, *Phys. Rev. Lett.* **111**, 060802 (2013).
 - [11] L. J. Fernández-Alcázar, R. A. Bustos-Marín, and H. M. Pastawski, Decoherence in current induced forces: Application to adiabatic quantum motors, *Phys. Rev. B* **92**, 075406 (2015).
 - [12] L. Y. Gorelik, A. Isacsson, M. V. Voinova, B. Kasemo, R. I. Shekhter, and M. Jonson, Shuttle Mechanism for Charge Transfer in Coulomb Blockade Nanostructures, *Phys. Rev. Lett.* **80**, 4526 (1998).
 - [13] T. Novotny, A. Donarini, and A.-P. Jauho, Quantum Shuttle in Phase Space, *Phys. Rev. Lett.* **90**, 256801 (2003).
 - [14] T. Novotný, A. Donarini, C. Flindt, and A.-P. Jauho, Shot Noise of a Quantum Shuttle, *Phys. Rev. Lett.* **92**, 248302 (2004).
 - [15] A. Donarini, T. Novotný, and A.-P. Jauho, Simple models suffice for the single-dot quantum shuttle, *New J. Phys.* **7**, 237 (2005).
 - [16] C. Flindt, T. Novotný, and A.-P. Jauho, Current noise spectrum of a quantum shuttle, *Phys. E (Amsterdam, Neth.)* **29**, 411 (2005).
 - [17] C. Kim, J. Park, and R. H. Blick, Spontaneous Symmetry Breaking in Two Coupled Nanomechanical Electron Shuttles, *Phys. Rev. Lett.* **105**, 067204 (2010).
 - [18] M. Prada and G. Platero, Double coupled electron shuttle, *Phys. Rev. B* **86**, 165424 (2012).
 - [19] C. Kim, M. Prada, G. Platero, and R. H. Blick, Realizing Broadbands of Strong Nonlinear Coupling in Nanoelectromechanical Electron Shuttles, *Phys. Rev. Lett.* **111**, 197202 (2013).
 - [20] R. I. Shekhter, L. Y. Gorelik, M. Jonson, Y. M. Galperin, and V. Vinokur, Nanomechanical shuttle transfer of electrons, *J. Comp. Theor. Nanosci.* **4**, 860 (2007).
 - [21] D. V. Scheible and R. H. Blick, A mode-locked nanomechanical electron shuttle for phase-coherent frequency conversion, *New J. Phys.* **12**, 023019 (2010).

- [22] B. Wang, L. Vuković, and P. Král, Nanoscale Rotary Motors Driven by Electron Tunneling, *Phys. Rev. Lett.* **101**, 186808 (2008).
- [23] A. Smirnov, L. Murokh, S. Savel'ev, and F. Nori, Biomimicking rotary nanodomotors, in *Nanotechnology IV* (International Society for Optics and Photonics, 2009), Vol. 7364, p. 73640D.
- [24] A. Croy and A. Eisfeld, Dynamics of a nanoscale rotor driven by single-electron tunneling, *Europhys. Lett.* **98**, 68004 (2012).
- [25] A. Celestino, A. Croy, M. Beims, and A. Eisfeld, Rotational directionality via symmetry-breaking in an electrostatic motor, *New J. Phys.* **18**, 063001 (2016).
- [26] C. W. Wächtler, P. Strasberg, and G. Schaller, Proposal of a Realistic Stochastic Rotor Engine Based on Electron Shuttling, *Phys. Rev. Appl.* **12**, 024001 (2019).
- [27] J. Echeverria, S. Monturet, and C. Joachim, One-way rotation of a molecule-rotor driven by a shot noise, *Nanoscale* **6**, 2793 (2014).
- [28] H.-H. Lin, A. Croy, R. Gutierrez, C. Joachim, and G. Cuniberti, Current-induced rotations of molecular gears, *J. Phys. Commun.* **3**, 025011 (2019).
- [29] T. Kudernac, N. Ruangsupapichat, M. Parschau, B. Maciá, N. Katsonis, S. R. Harutyunyan, K.-H. Ernst, and B. L. Feringa, Electrically driven directional motion of a four-wheeled molecule on a metal surface, *Nature (London)* **479**, 208 (2011).
- [30] F. D. Natterer, F. Patthey, and H. Brune, Distinction of Nuclear Spin States with the Scanning Tunneling Microscope, *Phys. Rev. Lett.* **111**, 175303 (2013).
- [31] T. Jung, R. Schlittler, and J. Gimzewski, Conformational identification of individual adsorbed molecules with the STM, *Nature (London)* **386**, 696 (1997).
- [32] A. Nickel, R. Ohmann, J. Meyer, M. Grisolia, C. Joachim, F. Moresco, and G. Cuniberti, Moving nanostructures: Pulse-induced positioning of supramolecular assemblies, *ACS Nano* **7**, 191 (2013).
- [33] H. L. Tierney, C. J. Murphy, A. D. Jewell, A. E. Baber, E. V. Iski, H. Y. Khodaverdian, A. F. McGuire, N. Klebanov, and E. C. H. Sykes, Experimental demonstration of a single-molecule electric motor, *Nat. Nanotechnol.* **6**, 625 (2011).
- [34] P. Mishra, J. P. Hill, S. Vijayaraghavan, W. V. Rossom, S. Yoshizawa, M. Grisolia, J. Echeverria, T. Ono, K. Ariga, T. Nakayama *et al.*, Current-driven supramolecular motor with *in situ* surface chiral directionality switching, *Nano Lett.* **15**, 4793 (2015).
- [35] B. Stipe, M. Rezaei, and W. Ho, Inducing and viewing the rotational motion of a single molecule, *Science* **279**, 1907 (1998).
- [36] G. Pawin, A. Z. Stieg, C. Skibo, M. Grisolia, R. R. Schlittler, V. Langlais, Y. Tateyama, C. Joachim, and J. K. Gimzewski, Amplification of conformational effects via tert-butyl groups: Hexa-tert-butyl decacyclene on Cu (100) at room temperature, *Langmuir* **29**, 7309 (2013).
- [37] F. Eisenhut, J. Meyer, J. Krüger, R. Ohmann, G. Cuniberti, and F. Moresco, Inducing the controlled rotation of single o-MeO-DMBI molecules anchored on Au (111), *Surf. Sci.* **678**, 177 (2018).
- [38] F. Pistolesi and R. Fazio, Charge Shuttle as a Nanomechanical Rectifier, *Phys. Rev. Lett.* **94**, 036806 (2005).
- [39] I. Giaever and H. Zeller, Superconductivity of Small Tin Particles Measured by Tunneling, *Phys. Rev. Lett.* **20**, 1504 (1968).
- [40] I. O. Kulik and R. I. Shekhter, Kinetic phenomena and charge-discreteness effects in granulated media, *Zh. Eksp. Teor. Fiz.* **68**, 623 (1975).
- [41] D. Averin and K. Likharev, Coulomb blockade of single-electron tunneling, and coherent oscillations in small tunnel junctions, *J. Low Temp. Phys.* **62**, 345 (1986).
- [42] See Supplemental Material at <http://link.aps.org/supplemental/10.1103/PhysRevResearch.3.L032020> which includes further details on the model and the numeric implementation, an analytic model for regime I, and the dependency of rectification on the driving frequency and on the temperature.
- [43] A. Celestino, Ph.D. thesis, Technische Universität Dresden, 2017.
- [44] C. W. Wächtler, P. Strasberg, S. H. L. Klapp, G. Schaller, and C. Jarzynski, Stochastic thermodynamics of self-oscillations: the electron shuttle, *New J. Phys.* **21**, 073009 (2019).